

Voxel-ICA for reconstruction of source signal time-series and orientation in EEG and MEG

Yaqub Jonmohamadi · Govinda Poudel ·
Carrie Innes · Richard Jones

Received: 29 August 2013 / Accepted: 19 March 2014 / Published online: 6 April 2014
© Australasian College of Physical Scientists and Engineers in Medicine 2014

Abstract In electroencephalography (EEG) and magnetoencephalography signal processing, scalar beamformers are a popular technique for reconstruction of the time-course of a brain source in a single time-series. A prerequisite for scalar beamformers, however, is that the orientation of the source must be known or estimated, whereas in reality the orientation of a brain source is often not known in advance and current techniques for estimation of brain source orientation are effective only for high signal-to-noise ratio (SNR) brain sources. As a result, vector beamformers are applied which do not need the orientation of the source and reconstruct the source time-course in three orthogonal (x, y, and z) directions. To obtain a single time-course, the vector magnitude of the three orthogonal outputs of the beamformer can be calculated at each time point (often called neural activity index, NAI). The NAI, however, is different from the actual time-course of a

source since it contains only positive values. Moreover, in estimating the magnitude of the desired source, the background activity (undesired signals) in the beamformer outputs also become all positive values, which, when added to each other, leads to a drop in the SNR. This becomes a serious problem when the desired source is weak. We propose applying independent component analysis (ICA) to the orthogonal time-courses of a brain voxel, as reconstructed by a vector beamformer, to reconstruct the time-course of a desired source in a single time-series. This approach also provides a good estimation of dipole orientation. Simulated and real EEG data were used to demonstrate the performance of voxel-ICA and were compared with a scalar beamformer and the magnitude time-series of a vector beamformer. This approach is especially helpful when the desired source is weak and the orientation of the source cannot be estimated by other means.

Y. Jonmohamadi · R. Jones
Department of Medicine, University of Otago, Christchurch,
New Zealand

Y. Jonmohamadi (✉) · G. Poudel · C. Innes · R. Jones
New Zealand Brain Research Institute, 66 Stewart Street,
Christchurch 8011, New Zealand
e-mail: jonya247@student.otago.ac.nz

G. Poudel
Monash Biomedical Imaging, Monash University, Melbourne,
Australia

C. Innes · R. Jones
Department of Electrical and Computer Engineering,
University of Canterbury, Christchurch, New Zealand

C. Innes · R. Jones
Department of Medical Physics and Bioengineering,
Christchurch Hospital, Christchurch, New Zealand

Keywords Beamformer · Electroencephalography ·
Independent component analysis ·
Magnetoencephalography · Signal-to-noise ratio ·
Time-course reconstruction

Introduction

Electroencephalography (EEG) and magnetoencephalography (MEG) are noninvasive procedures for measuring brain electric potentials or magnetic fields, respectively, by an array of sensors over the scalp. Compared with other common techniques in functional imaging of the brain, such as functional magnetic resonance imaging (fMRI) and positron emission tomography (PET), EEG and MEG have much higher temporal resolution and, therefore, provide an opportunity for localization and time-series reconstruction

of highly dynamic brain sources. The time-series of the sources provides information for investigation of the temporal dynamics of source activities and finding connectivity between sources. Therefore, techniques which can reconstruct the time-course of a source, especially under poor signal-to-noise ratio (SNR), such as beamforming, are in demand.

Beamforming is a popular technique for localization and signal reconstruction of brain sources in EEG and MEG [1–6] and their relative performances have been evaluated [7–10]. The beamformer is a form of spatial filtering for processing data from an array of sensors [4]. Beamformers were originally applied in array signal processing including sonar, radar, and seismic exploration [11]. In EEG and MEG, a beamformer can focus on any location in the brain and works so as to attenuate signals arising from other locations in the brain. Beamformers in EEG and MEG can be categorized into two types: (1) scalar beamformers and (2) vector beamformers. The scalar beamformer reconstructs the time-course of the source in a single time-series. In contrast, the vector beamformer reconstructs the time-course of a source in three orthogonal directions (x, y, and z). Hence, a scalar beamformer is more desirable. However, a prerequisite for scalar beamformers is that the orientation of the source is known or can be estimated. Differences between the actual orientation of the source and its presumed orientation degrade the performance of the beamformer [12, 13]. Therefore, techniques such as grid-search to maximize the source power [3, 14] or eigen-decomposition of the source power [4], with the largest eigenvalue corresponding to the source orientation for a given location, can be applied to estimate the source signal orientation. But in both approaches the power is assumed over a wide range (hundreds of ms) of EEG or MEG and it is assumed that only a single source is active for a given location. This assumption fails when the source of interest for a given location is weak and the time-series reconstructed for that location is mostly contributed to by a stronger interfering source outside the location of interest [15].

Hence, the application of scalar beamformers is confined to cases where the orientation of the source of interest is known or is the dominant source and its orientation can be estimated. In contrast, the vector beamformer does not require the orientation of the source. However, a difficulty with vector beamformers is that they cannot estimate the source time-series as a single signal. To obtain a single time-course, the vector magnitude of the three orthogonal outputs of the beamformer can be calculated at each time point [2, 4, 9] (often called neural activity index, NAI). The NAI, however, is different from the actual time-course of a source since it contains only positive values. Moreover, in estimating the magnitude of the desired source, the background activity (undesired signals) in the beamformer

outputs also become all positive values, which, when added to each other, leads to a drop in the SNR. This becomes a serious problem when the desired source is weak.

In this study, we reconstruct the time-courses of a given location by a vector beamformer and use independent component analysis (ICA) to (1) reconstruct the time-course of that location in a single time-series, (2) estimate the orientation of the source in the vicinity of that location, and (3) increase the SNR of the reconstructed signal. We then demonstrate that ICA is superior to NAI at each time sample for reconstructing the time-courses of brain source signals.

Throughout this paper, plain italics indicate scalars, lower-case boldface italics indicate vectors, and upper-case boldface italics indicate matrices. Subscript b refers to assumed location or orientation of the dipole and subscript d refers to actual location or orientation of the dipole.

Methods

Forward problem

The measured EEG or MEG signal $\mathbf{B}(t) = [\mathbf{b}(t_1), \mathbf{b}(t_2), \dots, \mathbf{b}(t_K)]^T$, K number of time samples, on M electrodes, at time point t is

$$\mathbf{b}(t) = \int \mathbf{L}(\mathbf{r}_d) \mathbf{q}_d(\mathbf{r}_d) s(t, \mathbf{r}_d) d(\mathbf{r}_d) + \boldsymbol{\eta}(t), \quad (1)$$

and $\mathbf{L}(\mathbf{r}_d) = [L_x(\mathbf{r}_d), L_y(\mathbf{r}_d), L_z(\mathbf{r}_d)]$ is a $M \times 3$ lead-field matrix which shows the sensitivity of scalp sensors in three orthogonal directions (x,y,z) to the source signal $s(t, \mathbf{r}_d)$ located at $\mathbf{r}_d = [r_{dx}, r_{dy}, r_{dz}]^T$ (mm) with a moment of $\mathbf{q}_d(\mathbf{r}_d) = [q_{dx}(\mathbf{r}_d), q_{dy}(\mathbf{r}_d), q_{dz}(\mathbf{r}_d)]^T$ (A.m), and $\boldsymbol{\eta}(t)$ is the additive noise. The dipole moment can be written as

$$\mathbf{q}_d(\mathbf{r}_d) = \alpha \tilde{\mathbf{q}}_d(\mathbf{r}_d), \quad \tilde{\mathbf{q}}_d(\mathbf{r}_d) = \mathbf{q}_d(\mathbf{r}_d) / \|\mathbf{q}_d(\mathbf{r}_d)\| \quad (2)$$

where $\tilde{\mathbf{q}}_d(\mathbf{r}_d)$ is the orientation of the dipole source and α is the magnitude of the dipole.

Scalar beamformer

The reconstructed time-course via a scalar beamformer for a given location \mathbf{r}_b and orientation \mathbf{q}_b is

$$\hat{s}(t, \mathbf{r}_b, \mathbf{q}_b) = \mathbf{w}^T(\mathbf{r}_b, \mathbf{q}_b) \mathbf{b}(t) \quad (3)$$

where $\mathbf{w}(\mathbf{r}_b, \mathbf{q}_b)$ is a $M \times 1$ vector of the scalar beamformer coefficients, $\mathbf{r}_b = [r_{bx}, r_{by}, r_{bz}]^T$ (mm) is assumed dipole location, and $\mathbf{q}_b(\mathbf{r}_b) = [q_{bx}(\mathbf{r}_b), q_{by}(\mathbf{r}_b), q_{bz}(\mathbf{r}_b)]^T$ is assumed dipole orientation. In the ideal case $\mathbf{q}_b = \tilde{\mathbf{q}}_d$. The orientation of the source must be known in advance, or, if not, needs to be estimated via orientation estimation algorithms [3, 4, 14].

However, although these algorithms work well when the source of interest is the dominant source, the estimation of \mathbf{r}_d will be inaccurate for small sources.

Vector beamformer

The reconstructed time-courses $\hat{\mathbf{s}}(t, \mathbf{r}_b) = [\hat{s}_x(t, \mathbf{r}_b), \hat{s}_y(t, \mathbf{r}_b), \hat{s}_z(t, \mathbf{r}_b)]$, of a source via a vector beamformer for a given location \mathbf{r}_b is

$$\hat{\mathbf{s}}(t, \mathbf{r}_b) = \mathbf{W}^T(\mathbf{r}_b)\mathbf{b}(t) \tag{4}$$

where $\mathbf{W}(\mathbf{r}_b) = [\mathbf{w}_x(\mathbf{r}_b), \mathbf{w}_y(\mathbf{r}_b), \mathbf{w}_z(\mathbf{r}_b)]$ is a $M \times 3$ matrix of the vector beamformer coefficients. In the case of MEG, it is possible to convert the three orthogonal reconstructed time-courses into two tangential (θ and ϕ) components and ignore the radial component as the radial component is effectively zero for MEG, by using Cartesian to spherical coordinate conversion [4].

One way to merge the three components of $\hat{\mathbf{s}}(t, \mathbf{r}_b)$ is to calculate the magnitude of the source at each time sample

$$|\hat{s}(t, \mathbf{r}_b)| = \sqrt{\hat{s}_x^2(t, \mathbf{r}_b) + \hat{s}_y^2(t, \mathbf{r}_b) + \hat{s}_z^2(t, \mathbf{r}_b)}. \tag{5}$$

Another approach is to estimate the NAI at each time sample. The NAI, however, has different formulations for different types of beamformers [9]. In this study, we focus on the vector minimum-variance (MV) beamformer, also known as the linearly-constrained minimum-variance (LCMV) beamformer, for which

$$NAI(t, \mathbf{r}_b) = \frac{\text{tr}\{\mathbf{W}^T(\mathbf{r}_b)\mathbf{b}(t)\mathbf{b}^T(t)\mathbf{W}(\mathbf{r}_b)\}}{\text{tr}\{(\mathbf{L}^T(\mathbf{r}_b)\mathbf{L}(\mathbf{r}_b))^{-1}\}} \tag{6}$$

where $\mathbf{W}(\mathbf{r}_b) = [\mathbf{w}_x(\mathbf{r}_b), \mathbf{w}_y(\mathbf{r}_b), \mathbf{w}_z(\mathbf{r}_b)]$ is the vector-MV beamformer weight matrix and

$$\mathbf{w}_\xi(\mathbf{r}_b) = \frac{\mathbf{C}^{-1}\mathbf{l}_\xi(\mathbf{r}_b)}{\mathbf{l}_\xi^T(\mathbf{r}_b)\mathbf{C}^{-1}\mathbf{l}_\xi(\mathbf{r}_b)}, \xi = x, y, z. \tag{7}$$

and \mathbf{C} is the covariance matrix

$$\mathbf{C} = \langle \mathbf{b}(t)\mathbf{b}^T(t) \rangle \tag{8}$$

where $\langle \dots \rangle$ is the ensemble average, and for the scalar-MV beamformer $\mathbf{w}(\mathbf{r}_b, \mathbf{q}_b)$ is

$$\mathbf{w}(\mathbf{r}_b, \mathbf{q}_b) = \frac{\mathbf{C}^{-1}\mathbf{l}(\mathbf{r}_b, \mathbf{q}_b)}{\mathbf{l}^T(\mathbf{r}_b, \mathbf{q}_b)\mathbf{C}^{-1}\mathbf{l}(\mathbf{r}_b, \mathbf{q}_b)} \tag{9}$$

where $\mathbf{l}(\mathbf{r}_b, \mathbf{q}_b)$ is the scalar lead-field

$$\mathbf{l}(\mathbf{r}_b, \mathbf{q}_b) = \mathbf{L}(\mathbf{r}_b)\mathbf{q}_b. \tag{10}$$

The NAI has been shown to be a superior option compared to magnitude $|\hat{s}(t, \mathbf{r}_b)|$ for measuring the activity of neural sources where the SNR of the source of interest is low [2]. If the normalized lead-field is used for the beamformer,

Eqs. (6) and (5) will be similar and the magnitude will become the square root of the NAI. Both $|\hat{s}(t, \mathbf{r}_b)|$ and $NAI(t, \mathbf{r}_b)$ have positive rectified values only and, therefore, the time-courses reconstructed by these two approaches are double the frequency of the original source signal $s(t, \mathbf{r}_d)$.

Voxel-ICA

ICA is a blind source separation technique. The concept of ICA lies in the fact that the signals may be decomposed into their constituent statistically independent components [16]. ICA has been successfully used for EEG signal processing, including component extraction of event-related potentials [17–21] and artefact removal [22, 23].

Voxel-ICA is proposed as a new technique to obtain a single time-series from three orthogonal time-series of vector beamformers and estimate the orientation of the source for a given location \mathbf{r}_b . Voxel-ICA is based on the application of ICA to the 3 orthogonal time-courses of a voxel (location \mathbf{r}_b), reconstructed via a vector beamformer. Ideally, the voxel should be close to the location of the source. Hence, a prerequisite of the voxel-ICA approach is that the approximate location of the source of interest must be known; i.e., $\mathbf{r}_b \approx \mathbf{r}_d$. ICA separates the time-course of the source of interest from other background activities which appear in the output of the vector beamformer leading to a higher SNR compared with NAI. The unmixing equation by ICA is

$$\mathbf{H}^T(\mathbf{r}_b)\hat{\mathbf{S}}(t, \mathbf{r}_b) = \bar{\mathbf{S}}(t), \tag{11}$$

where $\hat{\mathbf{S}}(t, \mathbf{r}_b)$ is the 3D orthogonal signal matrix after vector beamforming

$$\hat{\mathbf{S}}(t, \mathbf{r}_b) = \begin{pmatrix} \hat{s}_x(t_1, \mathbf{r}_b) & \hat{s}_x(t_2, \mathbf{r}_b) & \dots & \hat{s}_x(t_T, \mathbf{r}_b) \\ \hat{s}_y(t_1, \mathbf{r}_b) & \hat{s}_y(t_2, \mathbf{r}_b) & \dots & \hat{s}_y(t_T, \mathbf{r}_b) \\ \hat{s}_z(t_1, \mathbf{r}_b) & \hat{s}_z(t_2, \mathbf{r}_b) & \dots & \hat{s}_z(t_T, \mathbf{r}_b) \end{pmatrix}, \tag{12}$$

and $\mathbf{H}(\mathbf{r}_b) = [\mathbf{h}_1(\mathbf{r}_b), \mathbf{h}_2(\mathbf{r}_b), \mathbf{h}_3(\mathbf{r}_b)]$, $\mathbf{H}(\mathbf{r}_b) \in \mathfrak{R}^{(\times)}$ is the unmixing matrix and each of its columns is a unmixing vector for extracted independent components by ICA and each row of $\bar{\mathbf{S}}(t)$ is an independent component,

$$\bar{\mathbf{S}}(t) = \begin{pmatrix} \bar{s}_1(t_1) & \bar{s}_1(t_2) & \dots & \bar{s}_1(t_T) \\ \bar{s}_2(t_1) & \bar{s}_2(t_2) & \dots & \bar{s}_2(t_T) \\ \bar{s}_3(t_1) & \bar{s}_3(t_2) & \dots & \bar{s}_3(t_T) \end{pmatrix}. \tag{13}$$

By visual inspection it is possible to identify the time-course of the source of interest in $\bar{\mathbf{S}}(t)$. If $\bar{s}_i(t)$, $i = 1, 2, 3$ is the estimated time-course of the source of interest, then the orientation of the source is

$$\mathbf{q}_b(\mathbf{r}) = \mathbf{h}_i(\mathbf{r})/\|\mathbf{h}_i(\mathbf{r})\|, \quad i = 1, 2, 3. \tag{14}$$

Computer simulations

EEG setup and coordinates

Simulated EEG was synthesized by Eq. (1) and $\eta(t)$ was real background EEG. Real background EEGs were obtained from three healthy subjects in a resting state. The 64-channel 10–20 system was used for the location of EEG electrodes and the EEG was sampled at 250 Hz. Montreal Neurological Institute (MNI) coordinates are used to describe the locations in the brain. The boundary element method (BEM) model of the head [24] obtained from the average MNI-template brain, implemented in the FieldTrip toolbox [25], was used to calculate the lead-field matrix, with 3 layers and a conductivity ratio of skull to soft tissue of 0.0125. The directions of the x, y, and z axes are shown in Fig. 1. The length of the simulated EEG was 6 s. The EEGLAB toolbox [26] was used for ICA (infomax [27]).

Performance evaluation

To measure performance, the SNR of the reconstructed time-series by each approach was measured for a 1.0 s time window, 2.0–3.0 s. The FFT was used to measure the power of different frequencies and the SNR of the signal was calculated accordingly [10]. The SNR of the $d1$ and $d2$ sources superimposed on the real EEG was defined as the Frobenius norm of the source signal matrix to that of the real EEG matrix. To demonstrate the advantage of the voxel-ICA approach over NAI and a scalar beamformer, three situations were simulated:

- High SNR source: For this situation, the source of interest $d1$ had a relatively high SNR of 1.00. The spatial location and orientation of the $d1$ is shown in Fig. 2 and the time-course of the $d1$ is shown in Fig. 3.

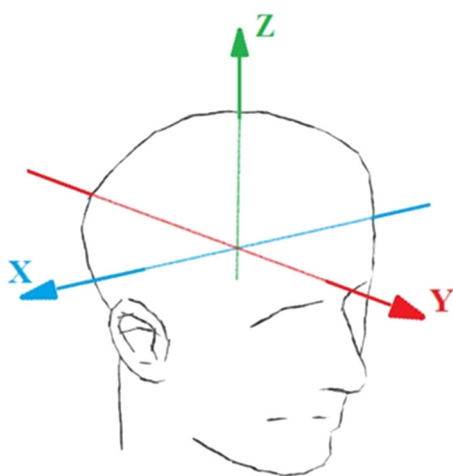


Fig. 1 The direction of the x, y, and z axes in the coordinate system used to describe the spatial location of the artificial dipole in the brain. Coordinate [0, 0, 0] is at the anterior commissure and in line with the anterior/posterior commissural line

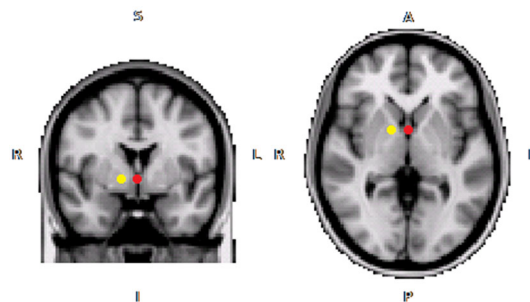


Fig. 2 The red dot shows the location of the source $s(t, \mathbf{r}_{d1})$, with $\mathbf{r}_{d1} = [0, 0, 0]^T$ mm and $\boldsymbol{\alpha}(\mathbf{r}_{d1}) = [0.57, 0.57, 0.57]^T$. The yellow dot shows the location of the interfering source $s(t, \mathbf{r}_{d2})$, with $\mathbf{r}_{d2} = [10, 0, 0]^T$ mm and $\boldsymbol{\alpha}(\mathbf{r}_{d2}) = [0.9, 0.0, 0.45]^T$

- Low SNR source: For this situation, the source of interest $d1$ had a small SNR of 0.20.
- Source located close to an interfering source: For this situation, while the source of interest $d1$ had a small SNR of 0.20, an interfering source $d2$ was placed nearby with a SNR of 0.50. For this part, the signal-to-interference ratio (SIR) [10] was measured for the scalar beamformer, NAI, and voxel-ICA, between 2 s and 3 s.

The accuracy of the estimated orientation of the desired dipole via voxel-ICA is given by the orientation error (OE):

$$OE = \arccos \frac{q_b \cdot \tilde{q}_d}{\|q_b\| \|\tilde{q}_d\|}. \quad (15)$$

Real EEG data

To compare the performances of voxel-ICA and NAI in a real-world situation, real EEG data from 128 scalp sensors, ActiveTwo system, were downloaded from the SPM website (<http://www.fil.ion.ucl.ac.uk/spm/data/mmfaces>). These EEG data contain 86 visual evoked potentials (VEPs).

Results

Figures 4, 5, and 6 show the reconstructed time-courses of the source $d1$ for three situations described in “Performance evaluation” section for Subject 1. Note that the magnitude of the time-series in these plots have been normalized for ease of visual comparison. The blue signals are the 3 orthogonal time-courses reconstructed by the vector-MV beamformer for which the assumed location of dipole for the beamformer was the actual location of the dipole (i.e., $\mathbf{r}_b = \mathbf{r}_{d1}$). The green signals are the three independent components found by ICA of the three orthogonal outputs of the vector-MV beamformer. The red

Fig. 3 The time-courses of the $d1$ and $d2$ sources. The sources are sinusoids of 8 Hz for $d1$ and 5 Hz for $d2$

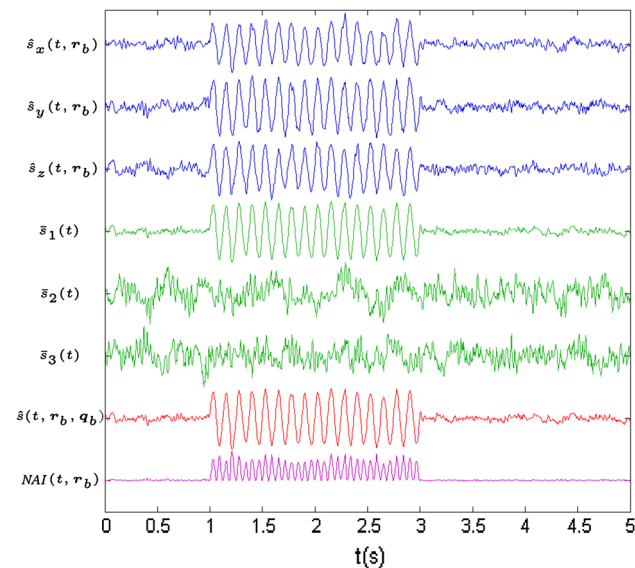
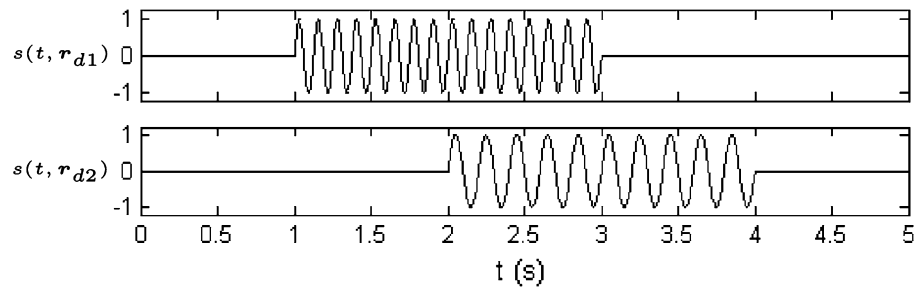


Fig. 4 The reconstructed and normalized time-courses of $d1$ with SNR = 1.0, via the vector-MV beamformer in blue, voxel-ICA in green, scalar-MV beamformer in red, and NAI in cyan. The SNRs of $\bar{s}_1(t)$, $\hat{s}(t, \mathbf{r}_b, \mathbf{q}_b)$, and $NAI(t, \mathbf{r}_b)$ are 81.9, 67.2, and 10.3 respectively. The orientation of $d1$ is $\mathbf{a}(r_{d1}) = [0.57, 0.57, 0.57]^T$ and the estimated dipole orientation via voxel-ICA for $\bar{s}_1(t)$, is $\mathbf{q}_b(r_{d1}) = [0.58, 0.64, 0.49]^T$

signal is the reconstructed time-course of $d1$ via the scalar-MV beamformer for which the assumed orientation for the beamformer was the actual orientation of the dipole (i.e., $\mathbf{q}_b = \mathbf{q}_{d1}$) and the cyan color signal is the reconstructed time-course of $d1$ via the NAI approach.

Based on Fig. 4, when the source of interest has a high SNR (i.e., ≥ 1), all three approaches—voxel-ICA, scalar beamformer, and NAI—work well and reconstruct the time-courses of source $d1$ with high SNRs, but NAI still has a lower SNR compared with the other two approaches. For a smaller magnitude source, however, Fig. 5 shows that, the NAI performs very poorly compared with voxel-ICA and the scalar beamformer. When source $d1$ was placed close to a stronger interfering source $d2$, again NAI had a very low SNR and SIR (Fig. 6).

Table 1 shows the results for voxel-ICA, scalar beamformer, and NAI for a source $d1$ placed close to a stronger interfering source $d2$, applied to background EEG of three subjects. Voxel-ICA had a performance, in terms of SNR

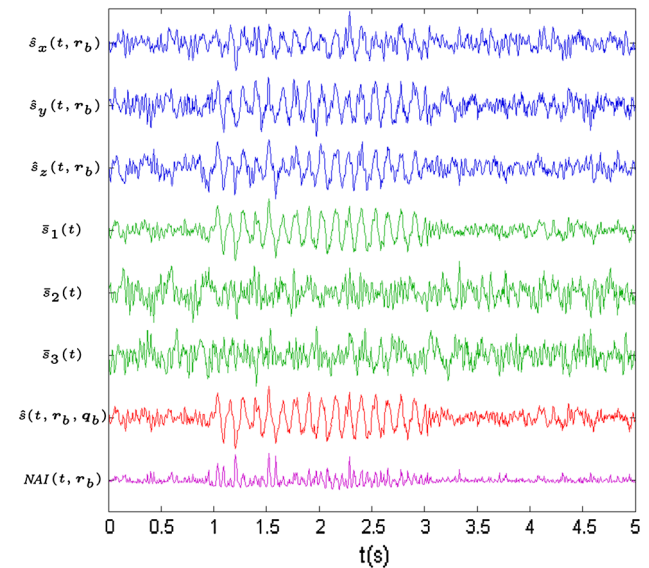


Fig. 5 The reconstructed and normalized time-courses of the source $d1$, SNR = 0.2, via the vector-MV beamformer in blue, voxel-ICA in green, scalar-MV beamformer in red, and NAI in cyan. The SNR of the $\bar{s}_1(t)$, $\hat{s}(t, \mathbf{r}_b, \mathbf{q}_b)$, and $NAI(t, \mathbf{r}_b)$ is 8.3, 8.2, and 0.6 respectively. The dipole orientation of $d1$ are $\mathbf{a}(r_{d1}) = [0.57, 0.57, 0.57]^T$ and the estimated dipole orientation via voxel-ICA for $\bar{s}_2(t)$, is $\mathbf{q}_b(r_{d1}) = [0.50, 0.60, 0.62]^T$

and SIR, which was only slightly less than that of the scalar beamformer with ideal orientation and outperforms the NAI. The table also shows the error that voxel-ICA had for estimated orientation of the desired source $d1$.

For the real EEG, VEPs, the location given to the beamformer was $[0 -65 16]$ mm, in the posterior region of the brain. As the orientation of the VEPs was not known in advance, the scalar beamformer could not be applied for this part and is shown as a flat red line in Fig. 7. The voxel-ICA approach, but not NAI at each time sample, was able to successfully separate the VEPs (component $\bar{s}_2(t)$ in Fig. 7) from other background activities. Also the artefact at 113.5 s appears strongly in NAI as well as orthogonal signals of the vector beamformer whereas voxel-ICA effectively separated this artefact from $\bar{s}_2(t)$. The circles in $\bar{s}_2(t)$ in Fig. 7 show the VEPs between each of the vertical dashed lines.

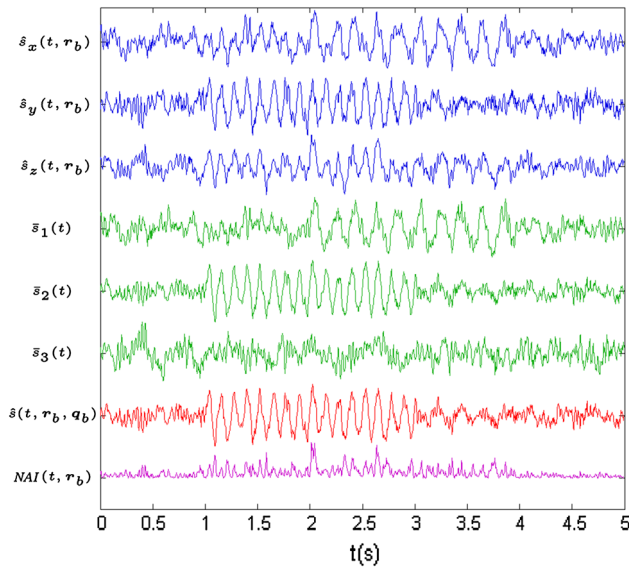


Fig. 6 The reconstructed and normalized time-courses of the source $d1$, with $\text{SNR} = 0.2$, in the presence of an interfering dipole ($d2$, $\text{SNR} = 0.5$) via the vector-MV beamformer in blue, voxel-ICA in green, scalar-MV beamformer in red, and NAI in cyan. The SNRs of $\bar{s}_2(t)$, $\hat{s}(t, \mathbf{r}_b, \mathbf{q}_b)$, and $\text{NAI}(t, \mathbf{r}_b)$ are 7.4, 7.5, and 0.6 respectively. The SIR of the $\bar{s}_2(t)$, $\hat{s}(t, \mathbf{r}_b, \mathbf{q}_b)$, and $\text{NAI}(t, \mathbf{r}_b)$ are 19.7, 15.8, and 1.6 respectively. The dipole orientation of $d1$ is $\boldsymbol{\eta}(\mathbf{r}_{d1}) = [0.57, 0.57, 0.57]^T$ and the interfering sources is $\boldsymbol{\eta}(\mathbf{r}_{d2}) = [0.70, 0.00, 0.70]^T$ the estimated dipole orientation via voxel-ICA, Eq. 14 for $\bar{s}_2(t)$, is $\mathbf{q}_b(\mathbf{r}_{d1}) = [0.16, 0.83, 0.52]^T$

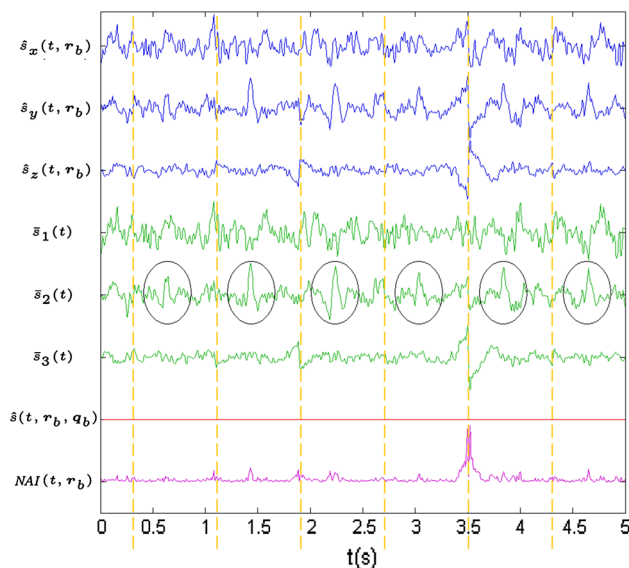


Fig. 7 The reconstructed and normalized time-courses of the VEPs, via the vector MV beamformer in blue, voxel-ICA in green, scalar-MV beamformer in red, and NAI in cyan. Component 2, $\bar{s}_2(t)$, is the component which represent the VEPs and the other two components are interfering sources. The estimated dipole orientation of VEPs via voxel-ICA, Eq. 14 for $\bar{s}_2(t)$, is $\mathbf{q}_b(\mathbf{r}_{d1}) = [0.20, 0.900, 0.37]^T$

Table 1 Measure of performance for a source located close to an interfering source applied on the EEG background of 3 subjects (SNR = signal-to-noise ratio, SIR = signal-to-interference ratio, OE = orientation error)

	Subject 1	Subject 2	Subject 3
Voxel-ICA			
SNR	7.4	6.0	7.8
SIR	15.8	8.4	10.3
OE	28°	24°	27°
Scalar beam-former			
SNR	7.5	6.3	7.9
SIR	19.7	13.4	13.0
NAI			
SNR	0.6	1.6	2.3
SIR	1.6	1.7	3.4

Voxel-ICA provided good estimation of dipole orientations, $\mathbf{q}_b(\mathbf{r}_{d1}) = [0.58, 0.64, 0.49]^T$ and $[0.50, 0.60, 0.62]^T$ for Fig. 4 ($\text{SNR} = 1.0$) and Fig. 5 ($\text{SNR} = 0.2$) respectively compared with the actual orientation of the source $\boldsymbol{\eta}(\mathbf{r}_{d1}) = [0.57, 0.57, 0.57]^T$, with $\text{OE} \approx 6^\circ$ for both cases. For the third situation in which the desired source was placed close to a stronger interfering source, the error of the estimated source orientation was larger at $\text{OE} \approx 26^\circ$ for all three background EEGs. However, voxel-ICA still provided a similar SIR and SNR to the scalar beamformer.

Discussion

We have proposed voxel-ICA as a means of reconstructing the time-course of a brain source in a single time-series with a high SNR for a given location. Voxel-ICA also provides an estimate of the orientation of the sources and the user does not need to use an exhaustive grid-search method [3, 14] or eigen-decomposition approach [4] which only work for high SNR sources.

A prerequisite of voxel-ICA is that the approximate location (i.e., ~ 10 mm) of the source of interest is known; if not, voxel-ICA can be applied to several locations in the subspace of interest to identify the desired source. If the user has no information on the location of sources of interest then source-space ICA [28] is recommended. Source-space ICA is a similar concept to voxel-ICA but, instead of one or several locations, it scans the whole brain and identifies the location, orientation, and time-course of the sources. However, source-space ICA requires considerably more computational time than voxel-ICA.

In the case of VEPs, the location given to the beamformer was $[0 -65 \ 16]$ mm whereas the location with the

highest power for VEPs was found (via vector-MV beamformer scanning) to be $[-2 \ -46 \ 28]$ mm and the voxel-ICA still worked well despite the location given to voxel-ICA being more than 20 mm away from the location of the primary VEPs source.

Voxel-ICA is especially useful when the desired source has a small SNR or is close to a strong interfering source. In such situations, NAI performs poorly (SNR and SIR at least three times smaller than voxel-ICA) and it may not be possible to use a scalar beamformer as the orientation of the source is unknown.

Estimation of source orientation after beamforming has been shown for radar and sonar for which a multi-rank beamformer is applied to a known subspace and singular value decomposition of the reconstructed time-series in the subspace provides information about the orientation of the sources [29, 30]. In comparison, voxel-ICA applies ICA for a single voxel or a cluster of voxels for a known location or subspace and is similar to the approaches described in [29, 30], except that ICA has been applied instead of singular value decomposition. In the current study, we focused on both the quality of the reconstructed time-series via voxel-ICA compared to other approaches and on voxel-ICA as a tool to identify source orientation.

Conclusion

Voxel-ICA involves the application of ICA following vector beamforming. In EEG and MEG, vector beamformers can be applied to reconstruct the time-courses of sources of interest. Vector beamformers provide three orthogonal outputs but the user is often interested in a single signal representing the source time-course. The NAI is also able to merge the three orthogonal outputs but the proposed voxel-ICA approach has been demonstrated to be superior both with simulated and real EEG sources. In addition to reconstruction of a source time-course, voxel-ICA is able to estimate source orientation.

Acknowledgments This work was funded by a University of Otago Postgraduate Scholarship. The authors thank Simon Knopp for his suggestions and thoughts on this work.

References

- Spencer M, Leahy RM, Mosher JC, Lewis PS (1992) Adaptive filters for monitoring localized brain activity from surface potential time series. *Proc IEEE Asilomar Conf Signal Syst Comput* 26:156–160
- Van Veen BD, van Drongelen W, Yuchtman M, Suzuki A (1997) Localization of brain electrical activity via linearly constrained minimum variance spatial filtering. *IEEE Trans Biomed Eng* 44:867–880
- Robinson SE, Vrba J (1998) Functional neuroimaging by synthetic aperture magnetometry (SAM). *Proceedings of the 11th International Conference on Biomagnetism* pp. 302–305
- Sekihara K, Nagarajan SS, Poeppel D, Marantz A, Miyashita Y (2001) Reconstructing spatio-temporal activities of neural sources using an MEG vector beamformer technique. *IEEE Trans Biomed Eng* 48:760–771
- Ward DM, Jones RD, Bones PJ, Carroll GJ (1999) Enhancement of deep epileptiform activity in the EEG via 3-D adaptive spatial filtering. *IEEE Trans Biomed Eng* 46:707–716
- Congedo M (2006) Subspace projection filters for real-time brain electromagnetic imaging. *IEEE Trans Biomed Eng* 53:1624–1634
- Greenblatt RE, Ossadtchi A, Pfeieger ME (2005) Local linear estimators for the linear bioelectromagnetic inverse problem. *IEEE Trans Biomed Eng* 53:3403–3412
- Sekihara K, Sahani M, Nagarajan SS (2005) Localization bias and spatial resolution of adaptive and non-adaptive spatial filters for MEG source reconstruction. *NeuroImage* 25:1056–1067
- Huang MX, Shih JJ, Lee RR, Harrington DL, Thoma RJ, Weisend MP, Hanlon F, Paulson KM, Li T, Martin K, Millers GA, Canive JM (2004) Commonalities and differences among vectorized beamformers in electromagnetic source imaging. *Brain Topogr* 16:139–158
- Mohamadi YJ, Poudel G, Innes C, Jones R (2012) Performance of beamformers on EEG source reconstruction. *Proc Int Conf IEEE Eng Med Biol Soc* 34:2517–2521
- Van Veen BD, Buckley KM (1988) Beamforming: a versatile approach to spatial filtering. *IEEE Mag Acoust Speech Signal Process* 5:4–24
- Li J (2005) *Robust adaptive beamforming*. Wiley, Hoboken
- Sekihara K, Nagarajan SS, Poeppel D, Marantz A (2004) Asymptotic SNR of scalar and vector minimum-variance beamformers for neuromagnetic source reconstruction. *IEEE Trans Biomed Eng* 51:1726–1734
- Vrba J, Robinson SE (2001) Signal processing in magnetoencephalography. *Methods* 25:249–271
- Quraan MA (2011) Characterization of brain dynamics using beamformer techniques: advantages and limitations. In: Pang EW (ed) *Magnetoencephalography*. InTech, Toronto, pp 67–92
- Sanei S, Chambers JA (2007) *EEG signal processing*. Wiley, West Sussex
- Onton J, Westerfield M, Townsend J, Makeig S (2006) Imaging human EEG dynamics using independent component analysis. *Neurosci Biobehav Rev* 30:808–822
- Makeig S, Debener S, Onton J, Delorme A (2004) Mining event-related brain dynamics. *Trends Cogn Sci* 8:204–210
- Jervis B, Belal S, Camilleri K, Cassar T, Bigan C, Linden D, Michalopoulos K, Zervakis M, Besleaga M, Fabri S, Muscat J (2007) The independent components of auditory P300 and CNV evoked potentials derived from single-trial recordings. *Physiol Meas* 28:745–771
- Ventouras EM, Ktonas PY, Tsekou H, Paparrigopoulos T, Kalatzis I, Soldatos CR (2010) Independent component analysis for source localization of EEG sleep spindle components. *Comput Intell Neurosci* 2010:1–12
- La Foresta F, Mammone N, Morabito FC (2009) PCAICA for automatic identification of critical events in continuous coma-EEG monitoring. *Biomed Signal Process Control* 4:229–235
- Jung TP, Humphries C, Lee TW, Makeig S, McKeown MJ, Iragui V, Sejnowski TJ (1998) Extended ICA remove artifacts from electroencephalographic recordings. *Adv Neural Inf Process Syst* 10:894–900
- Jung TP, Makeig S, Humphries C, Lee TW, McKeown MJ, Iragui V, Sejnowski TJ (2000) Removing electroencephalographic artifacts by blind source separation. *Psychophysiology* 37:163–178

24. Oostendorp TF, van Oosterom A (1989) Source parameter estimation in inhomogeneous volume conductors of arbitrary shape. *IEEE Trans Biomed Eng* 36:382–391
25. Oostenveld R, Fries P, Maris E, Schoffelen JM (2011) Fieldtrip: open source software for advanced analysis of MEG, EEG, and invasive electrophysiological data. *Comput Intell Neurosci* 2011:1–9
26. Delorme A, Makeig S (2004) EEGLAB: an open source toolbox for analysis of single-trial EEG dynamics. *J Neurosci Methods* 134:9–21
27. Bell AJ, Sejnowski TJ (1995) An information-maximization approach to blind separation and blind deconvolution. *Neural Comput* 7:1129–1159
28. Jonmohamadi Y, Poudel G, Innes C, Jones R (2013) Electromagnetic tomography via source-space ICA, *Proc Int Conf IEEE Eng Med Biol Soc* 35:37–40
29. Pezeshki A, Van Veen BD, Scharf LL, Cox H (2008) Eigenvalue beamforming using a multirank MVDR beamformer and subspace selection. *IEEE Trans Signal Process* 56:1954–1967
30. Scharf LL, Pezeshki A, Van Veen BD, Cox H, Besson O (2006) Eigenvalue beamforming using a multirank MVDR beamformer and subspace selection. *Proceedings of 5th Workshop on Defence Application of Signal Process*, Queensland, Australia, 10–14 Dec 2006